BMC Bioinformatics

RESEARCH

Open Access

ORFeus: a computational method to detect programmed ribosomal frameshifts and other non-canonical translation events

Mary O. Richardson[1] and Sean R. Eddy[1,2*]

*Correspondence:
seaneddy@fas.harvard.edu

[1] Department of Molecular and Cellular Biology, Harvard University, Cambridge, MA, USA
[2] Howard Hughes Medical Institute, Harvard University, Cambridge, MA, USA

Abstract

Background: In canonical protein translation, ribosomes initiate translation at a specific start codon, maintain a single reading frame throughout elongation, and terminate at the first in-frame stop codon. However, ribosomal behavior can deviate at each of these steps, sometimes in a programmed manner. Certain mRNAs contain sequence and structural elements that cause ribosomes to begin translation at alternative start codons, shift reading frame, read through stop codons, or reinitiate on the same mRNA. These processes represent important translational control mechanisms that can allow an mRNA to encode multiple functional protein products or regulate protein expression. The prevalence of these events remains uncertain, due to the difficulty of systematic detection.

Results: We have developed a computational model to infer non-canonical translation events from ribosome profiling data.

Conclusion: ORFeus identifies known examples of alternative open reading frames and recoding events across different organisms and enables transcriptome-wide searches for novel events.

Keywords: Non-canonical ORF, Alternative ORF, Ribosome profiling, HMM

Background

Deviation from the rules of canonical protein translation can lead to protein synthesis from alternative ORFs (altORFs). Altered initiation may result in upstream ORFs (uORFs) or downstream ORFs (dORFs) [1, 2]. Elongation and termination can be affected by a a category of alternative translational events termed recoding events, where the usual rules of mRNA decoding are altered. Recoding events during elongation include programmed ribosomal frameshifting (PRF), where the ribosome slips forward or backward (usually by + 1 or − 1 nucleotide) and changes reading frame during translation [3, 4]. Recoding events during termination include stop codon readthrough (SCR) or incorporation of selenocysteine or pyrrolysine, which lead to extended translation past an in-frame stop codon [5, 6]. These non-canonical and recoding events generate alternate protein sequences and are an important feature of the translational landscape

of many organisms. Alternative translation events, especially frameshifts, are common in viruses [7], but alternate translation mechanisms are also observed beyond viruses, from bacteria to humans. It is increasingly clear that these events may be more widespread than we realize, with known examples spanning all domains of life [8–17]. Non-canonical and recoding events can act as a regulatory switch for protein synthesis or can enable synthesis of multiple different functional protein products from a single mRNA. Together, frameshifts and other non-canonical events play an important role in regulating translation and producing alternate peptides that may have gone undetected using standard annotation pipelines.

One method for detecting these alternate translation events is ribosome profiling (ribo-seq). Ribo-seq is a technique that provides nucleotide-resolution information about ribosome position during translation, which can be used to infer open reading frames (ORFs). The protocol for ribo-seq involves (i) treating ribosome-bound mRNAs with a nuclease—typically RNase I or micrococcal nuclease (MNase), (ii) isolating the ribosome-protected fragments (or 'footprints') (iii) generating a library for deep sequencing, and (iv) mapping the ribosome footprints back to the genome or transcriptome [18]. The pattern of mapped reads can then be used to identify translated regions by manually or computationally searching for regions of high read density. In many ribo-seq data sets (though not all), aggregate ribosome footprint density over coding genes shows a characteristic triplet periodicity. This periodicity suggests that ribo-seq data can not only be used to measure ribosome density in an ORF at course resolution, but also to measure the reading frame that ribosomes are in at nucleotide resolution.

However, this requires looking at the data one ORF at a time, and at the single-ORF level the signal is often much more sparse. While some nucleotide (nt) positions have a high footprint density, the majority of positions in an mRNA typically have no mapped footprints. This heterogeneity presents a challenge for directly inferring frame at each nt position of a gene. Ribo-seq data can also exhibit a high level of noise, due in part to nuclease sequence bias and variability in footprint length [19]. This is especially pronounced in initial work in bacteria, where the wide range of footprint lengths blurs the signal and makes it difficult to decipher which nucleotide is in the P-site. However, subsequent work has demonstrated that adding the endonuclease RelE (in addition to MNase) during ribosome profiling in *E. coli* results in clear triplet periodicity of footprint ends (in aggregated metagenes) [20]. Additionally, computational approaches have been developed to determine the position of the P-site within different length ribo-seq fragments, which improves resolution for data sets generated with MNase, RNase I, or other nucleases [21].

Numerous methods exist to detect ORFs from ribo-seq data based on the distribution, periodicity, or read lengths of footprints in actively translated regions. Many of these algorithms allow for detection of novel ORFs, alternative initiation, and short uORFs or dORFs [22–33]. Some allow for ORFs with non-AUG start codons. However, current methods fall short when searching for recoding events that break the rules of canonical translation. Recoding events like programmed ribosomal frameshifts and stop codon readthrough violate the assumptions of current models, making detection difficult. Ribo-seq data has the power to reveal these recoding events [16, 34, 35], but there is no integrated approach available. Incorporating detection of alternative ORFs (altORFs)

and recoding events into a single method would allow for a more complete annotation process and help flag unexpected translation events for investigation.

Here we present ORFeus, a novel computational tool for inferring altORFs. ORFeus uses a hidden Markov model (HMM) to infer translation patterns from ribo-seq data that is inherently noisy and sparse. HMMs have been used for detection of translated ORFs from ribo-seq data previously by RiboHMM [22]. RiboHMM is an HMM-based ORF detector that predicts canonical ORFs from ribo-seq data, but this tool is limited to detection of a single canonical ORF per transcript and does not consider the possibility of frameshifts or stop codon readthrough. Separately, HMMs have also been used to infer frameshifts from nucleotide sequence by GeneTack [36]. Here we propose an HMM architecture designed to detect multiple types of recoding and alternative events using ribo-seq data in conjunction with nucleotide sequence. ORFeus identifies changes in reading frame and additional upstream or downstream reading frames. Given high coverage, periodic ribo-seq data, ORFeus can identify novel or extended ORFs (including uORFs and dORFs) with either canonical or alternative start codons, as well as programmed ribosomal frameshifts and stop codon readthrough events.

Results

Data processing

ORFeus takes as input aligned ribosome profiling data, reference annotations, and a reference genome sequence. The annotations file should contain known 5'UTR, 3'UTR, and protein-coding ORF features (although for bacteria, UTRs are typically not annotated). Aligned ribo-seq reads submitted to ORFeus should be uniquely mapped to the genome and have their 5' ends (or 3' ends) offset to correspond to the P-site of the ribosome (see Methods for further explanation) (Fig. 1A). Mapping reads uniquely to the genome is advised (though not strictly required) to avoid confounding signal from multimapped reads that may be mistaken for alternative translation. Available tools for alignment and pre-processing include RiboGalaxy [37] and Shoelaces [21].

The first step performed by ORFeus is a data processing step to combine information from the input aligned ribosome profiling data, reference annotations, and reference genome sequence. During this data processing step, ORFeus associates each protein-coding transcript (5'UTR, ORF, and 3'UTR) to its aligned ribo-seq read counts and nucleotide sequence using the annotations and genome sequence. For bacteria, we split the genome into one "transcript" per protein-coding ORF (each "transcript" corresponds directly to one annotated ORF plus any annotated UTRs in the upstream/downstream intergenic regions); i.e. we ignore operon structure and analyze one ORF at a time. To control for variation in both length and expression across different transcripts, ORFeus converts input read counts to relative ribo-seq density, which we call ρ. The relative ribo-seq density ρ_i^t at position i of transcript t is calculated by normalizing the raw read counts at position i of transcript t by the mean read counts per position for transcript t: $\rho_i^t = c_i^t / \bar{c_t}$. This per-transcript normalization ensures that ribo-seq density values are comparable across different transcripts, so the model can expect similar magnitude ρ_i^t values within each translated ORF. Note, however that transcripts with especially long UTRs with no coverage will have lower $\bar{c_t}$, and thus higher ρ_i^t relative to transcripts with

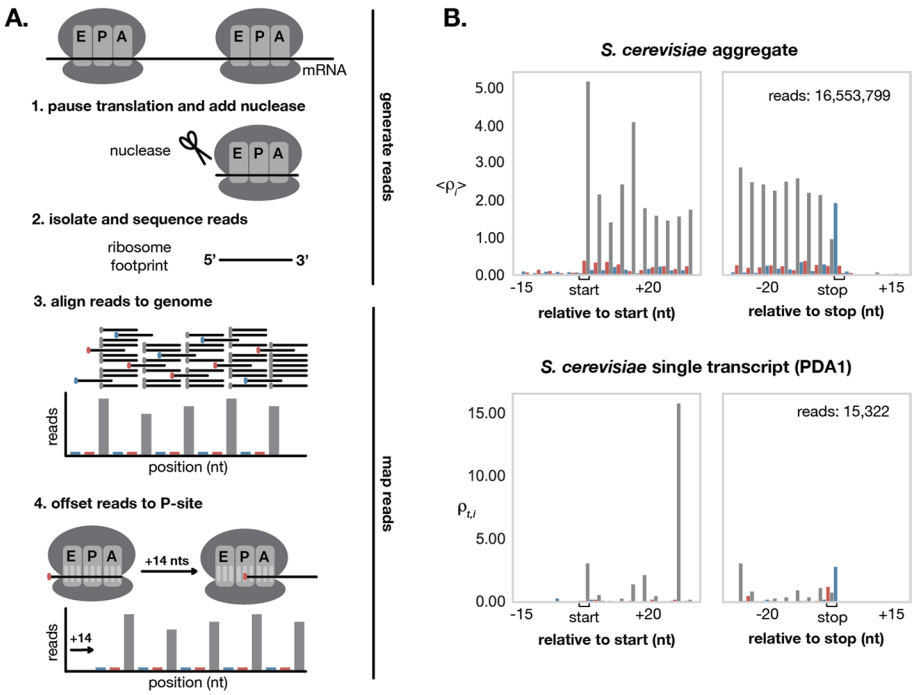

Fig. 1 Processing ribo-seq data. **A** Ribo-seq involves experimentally generating reads (top), then computationally mapping sequenced reads to precise ribosome positions (bottom). Ideal data shows a clear triplet periodicity and can be offset to correspond to a position within the P-site of the ribosome by shifting the 5′ or 3′ end of all reads. **B** Realigned ribo-seq data from Wu et al [38] shows clear triplet periodicity in aggregate across all annotated ORFs in *S. cerevisiae* (top). This periodic pattern is not as obvious in individual ORFs (bottom). The ribo-seq signal shown here for PDA1, a housekeeping gene commonly used as a reference in gene expression studies, is representative of the signal observed across other genes in *S. cerevisiae*

short or no UTRs. When aggregated across all transcripts, ideal ribo-seq density values should be near zero in the UTRs and exhibit clear periodicity within the ORFs (Fig. 1B).

ORFeus algorithm

ORFeus is designed to detect both canonical and non-canonical ORFs from ribo-seq data (Fig. 2A). It uses a hidden Markov model (HMM) trained to recognize ribo-seq signal and nucleotide sequence features characteristic of translated ORFs. HMMs provide a probabilistic framework well-suited for handling noisy and sparse signals like ribo-seq data [39]. An HMM predicts the most probable path of hidden "states" that could generate the observed data. In our case, ORFeus takes as input information about the ribo-seq reads and nucleotide sequence at each position of a transcript and returns the most likely path of ORF or non-ORF states for that transcript.

A simple HMM to model a canonical ORF includes eleven types of states: a 5'UTR state, a 3'UTR state, and states corresponding to nucleotide 1, 2, and 3 of each start codon, sense codon, and stop codon. The simple model (Fig. 2B) generates ribo-seq ρ_i^t values for each position in the transcript. There is additional information in the nucleotide sequence of the transcript, including codon usage preferences and start/stop codon preferences. To accommodate this codon information in the HMM, we expand the model to also emit a nucleotide for each state. The resulting model includes separate

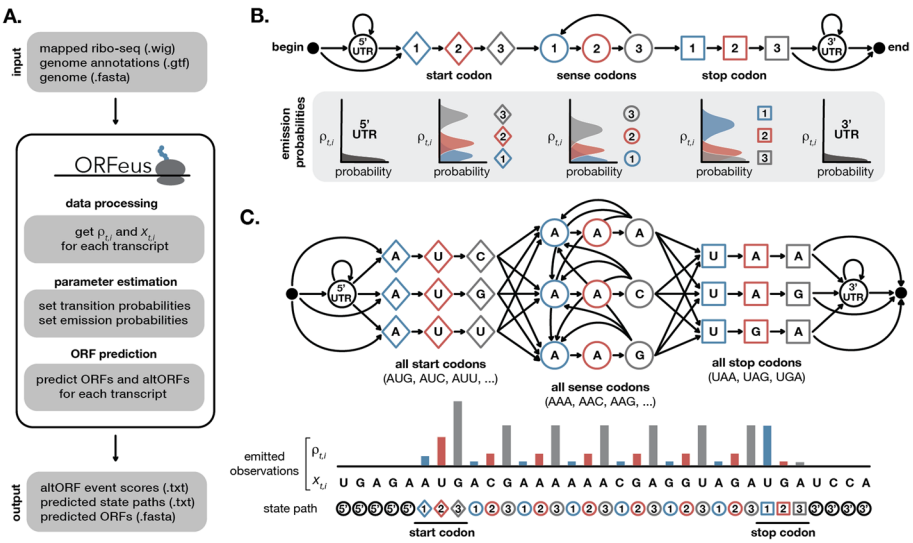

Fig. 2 Inferring canonical ORFs from ribo-seq data. **A** ORFeus takes in mapped ribo-seq data, genome annotations, and genome sequences and returns predicted ORFs calculated using an HMM. **B** A simple HMM to model canonical translation includes states corresponding to the 5'UTR and 3'UTR as well as nucleotide 1 (blue), 2 (red), and 3 (grey) of each start codon (diamonds), sense codon (circles), and stop codon (squares). All nonzero transition probabilities are denoted with arrows. A schematic representation of the emission probabilities for each state are plotted below the corresponding states. **C** A more complex HMM includes states for each individual start, stop, and sense codon sequence. Idealized ribo-seq density for a transcript that undergoes canonical translation of a single ORF is depicted below the model. The input relative ribo-seq density ρ_i^t and nucleotide sequence x_i^t at each position inform the output state path prediction

trios of states for each possible start, sense, and stop codon. Only single (P-site) codon states are modeled, but alternate model architectures could include states for each possible pair of (A-site and P-site) codons. We chose to include only single codons in order to limit the number of total states and constrain model complexity. Our simple canonical ORF model (Fig. 2C) generates two observed sequences: the ribo-seq values ρ_i^t and the nucleotide sequence x_i^t. Valid start codons are determined by default from the annotations and genome sequence files, but can be altered by the user. This enables non-AUG start codon detection.

To model non-canonical ORFs, we add additional states and transitions (Fig. 3A). Our original goal was just to capture programmed ribosomal frameshifts. To model a $+1$ frameshift we added an X_1 state to represent the nucleotide that is skipped over during translation. Translation can then resume in the $+1$ reading frame, continuing to a sense codon nucleotide 1 state (Fig. 3A blue arrows). We then chose to model a -1 frameshift as a $+2$ frameshift, since the resulting downstream frame should be equivalent and this is a reasonable approximation given the resolution of ribo-seq data. To shift the reading frame forward by two nucleotides (equivalent to back by one nucleotide), we added a second state X_2 to represent the second nucleotide that is skipped over during a $+2$ frameshift (Fig. 3A red arrows).

Since the HMM framework is very general, we can also add states and transitions to capture additional alternative translation events. We added stop codon readthrough by allowing movement from a stop codon directly back to a new sense codon (Fig. 3A purple arrow). To model short upstream and downstream ORFs, we added special start,

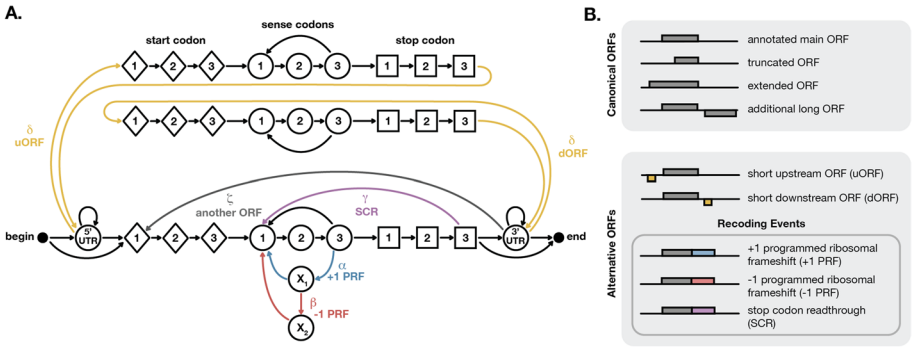

Fig. 3 Inferring alternative ORFs from ribo-seq data. **A** A more complex HMM to model non-canonical translation includes additional states and transitions to represent upstream ORFs and downstream ORFs (yellow), programmed ribosomal frameshifting (blue and red), and stop codon read-through (purple). The probability of each type of event (denoted with a Greek letter) is set to reflect its expected frequency. **B** The full model can infer both canonical ORFs and alternative ORFs, including recoding events

sense, and stop codon states that can be accessed only from within the 5'UTR or 3'UTR respectively (Fig. 3A yellow arrows). These uORF and dORF states are included as separate states from the main ORF since their lengths are expected to be much shorter. Multiple long ORFs are included by allowing a transition from a 3'UTR into another main ORF (Fig. 3A grey arrow). The full model predicts several types of canonical and non-canonical translation (Fig. 3B).

Parameter estimation

After the ribo-seq data has been processed, ORFeus is trained on the input data set to recognize the signals for ORF and non-ORF states, with data-specific parameters. There are two sets of probabilities that must be estimated:

- *Transition probabilities* represent the probability of moving to state k from state $k-1$. These are represented by arrows in Fig. 2B, C. For example, the probability of moving from a 5'UTR state into a start codon state is represented by the arrow from the 5'UTR state to the start nucleotide 1 state.
- *Emission probabilities* represent the probability of observing a specific ribo-seq value ρ_i^t and nucleotide x_i^t in state k. Different states have different expected ribo-seq density values. These are represented by rotated histograms below the state map in Fig. 2C. For example, we expect mostly $\rho_i^t = 0$ for positions in the 5'UTR state (dark grey histogram below the 5'UTR state), while we expect to observe higher ρ_i^t values more often for positions in start codon states (blue, red, and light grey histograms below the start codon). The nucleotide identity also factors into the emission probabilities for the expanded model shown in Fig. 2C, since only some nucleotides are allowable for certain states (e.g. UAA, UAG, and UGA for stop codons). Most states emit their designated nucleotide x_i^t with probability 1.0. However, UTR states can emit any nucleotide with equal probability.

The input annotations are used to determine the bounds of each mRNA transcript associated annotated canonical ORFs. Only the annotated canonical ORFs are used

to estimate the model parameters for canonical ORF states. The probabilities for non-canonical ORF states are derived from these canonical ORF parameters or set manually as described below. We exclude known non-canonical events from the training and instead test on these events to evaluate model performance.

Transition probabilities

Except for the few transitions discussed below, the transition probabilities are set to the observed frequency of each type of transition, based on the input transcriptome (generated from the annotations and genome sequence as described in data processing). For example, the probability of transitioning from the begin state into a 5'UTR is proportional to the frequency of annotated transcripts with 5'UTRs in the input transcriptome. The probability of remaining in a 5'UTR versus transitioning to a start codon is based on the mean length of annotated 5'UTRs. The probability of moving from the 5'UTR into state 1 of a particular start codon also depends on the relative frequency of this start codon across all annotated transcripts. Similarly, the probability of moving from state 3 of one sense codon to state 1 of the next sense codon is the relative usage of this next codon across all annotated transcripts. In this way, most of the model's transitions are set to reflect features specific to the input transcriptome. All transition probabilities are enumerated in Additional file 1: Table S1.

There are six transition probabilities that are set to the expected frequency of non-canonical translation events (denoted by Greek letters in Fig. 3A). These six probabilities, which we call altORF event parameters, are set by hand. We have little a priori knowledge of the rate of multiple ORFs, stop codon readthrough, or programmed ribosomal frameshifting across transcriptomes, and we cannot estimate them from the annotations, so we set these values instead by optimizing correct identification of known events across our test data sets. We chose a single set of values that worked to identify known events across all of our test data sets. The probability of frameshifting per codon $\alpha = 10^{-5}$ is the total probability of a programmed ribosomal frameshift event, either in the $+1$ or -1 direction. The probability of -1 frameshift given that a frameshift occurs $\beta = 0.5$ represents the relative frequency of $+1$ and -1 frameshifting (thus we assume that both types of frameshifting are equally likely). The probability of stop codon readthrough per ORF $\gamma = 10^{-4}$ is the total probability of translation past an in-frame stop codon, whether by sense codon incorporation or stop codon bypassing. The probability of short ORFs (including uORFs and dORFs) $\delta = 10^{-3}$ is the probability of observing a short ORF at each nucleotide in the 5'UTR or 3'UTR. The probability of multiple non-overlapping ORFs $\zeta = 10^{-10}$ is the probability of initiating another long ORF (including longer uORFs and dORFs) at each 3'UTR position downstream of the main ORF. Each of these parameters can be adjusted by the user to more accurately reflect the expected probabilities of alternative translation in the transcriptome of interest.

Emission probabilities

The emission probabilities are set to the probability of observing a particular nucleotide and a particular relative ribo-seq density ρ_i^t value in each state. The total emission probability is therefore the product of the nucleotide emission probability and

the ribo-seq emission probability. We emit both values at each state so that the model is informed by both ribo-seq and nucleotide sequence.

The nucleotide emission probability is one over the number of possible nucleotides if the nucleotide is represented by this state, and zero otherwise. For most states, only a single nucleotide can be emitted, so this value is 1 for that nucleotide. However, some states (including UTR states) can emit any nucleotide. For example, the probability of observing A, T, C, or G in a UTR state is 1/4, since any valid nucleotide may be represented by these states (and we chose not to incorporate information about UTR nucleotide composition to avoid biasing our search against finding novel ORFs in annotated UTRs). In contrast, the probability of observing A in an ACG1 sense codon state is 1, since the first nucleotide state of an ACG codon must be an A.

The ribo-seq emission probability is calculated for each state using the frequency of ρ_i^t observed across all annotated protein-coding transcripts. For example, the probability of observing $\rho_i^t = 0.5$ in an ACG1 state is set to the frequency of $\rho_i^t = 0.5$ values across all first positions of annotated ACG sense codons. The ribo-seq emission histograms are binned to speed up downstream calculations, with 25 uniform bins spanning the range of observed ρ_i^t values in the input ribo-seq data.

Since each start, sense, and stop state represents a single codon, certain differences in signal that are sequence-specific can be picked up by the model. For example, some nucleases used in ribosome profiling can exhibit nucleotide bias, preferentially cleaving after certain nucleotides leading to added noise. For example, RelE usually cleaves after the second nucleotide of the A-site, but prefers to cleave after a C nucleotide (and strongly avoids cleavage before a C nucleotide) [20]. As a result, NNC codons are more often cleaved after the third nucleotide of the A-site instead, leading to a disruption in periodicity at these codons [20]. The codon-specific emissions in our model recognize this bias, expecting to see density at the third nucleotide in NNC codons and the second nucleotide in other codons. This strategy turns some types of nuclease bias into signal that the model can use to inform reading frame prediction. This is useful in all cases except for especially small transcriptomes (such as viral or organellar transcriptomes). When there are too few transcripts to train emissions for each possible codon, we suggest pooling all codons during calculation of the emissions, which is an option available to the user.

The emissions for non-canonical ORF states are set after the canonical ORF emissions have been calculated. The emissions for uORF and dORF states are set to be the same as those for a canonical ORF. The emissions for the frameshift states X_1 and X_2 are naively set to the mean of the emissions for states 1, 2, and 3, since we have no prior knowledge about what these distributions should look like (since known frameshifts are rare).

After estimating all emission probabilities, we add a pseudocount of 10^{-10} to each ribo-seq emission probability bin and then re-normalize so that the total emission probability for each state is still one. This ensures that there is a non-zero probability of observing any possible ribo-seq value in each state. The advantage of this is that it allows the model to consider paths that go through unlikely (but not impossible) states for a given sequence and lets the model predict ORFs that contain ribo-seq values that were not observed in annotated ORFs for the given data set.

ORF prediction

After the parameters have been trained, ORFeus is ready to predict ORFs for individual transcripts. For a single transcript, ORFeus returns the most probable state path. This indicates the positions and sequences of predicted canonical and non-canonical ORFs. We use the Viterbi algorithm [40] to compute the most probable state path for each transcript.

The output path tells us whether an altORF is inferred. The predicted state path for a $+1$ frameshift event includes state X_1, which shifts the downstream frame forward by one nucleotide. The predicted state path for a -1 frameshift (or $+2$ frameshift) event includes states X_1 and X_2, which shifts the downstream frame forward by two nucleotides (which is is equivalent to shifting the downstream frame backward by one nucleotide). Similarly, the presence of uORF or dORF states indicates multiple ORFs are predicted and gives the exact inferred sequence of these additional ORFs. Finally, to indicate stop codon readthrough, the Viterbi path includes the transition from a stop state 3 back to sense state 1.

Model testing

Known altORFs

To test ORFeus, we ran the model on known examples of alternative translation that were held out from the training annotations. We used examples from multiple species to evaluate the method, which can be run on data from varied organisms and ribo-seq experimental protocols. We trained and ran the model on published data from *E. coli* [20], *S. cerevisiae* [38], *D. melanogaster* embryos [16], *D. rerio* embryos [31], and SARS-CoV-2 infected *C. sabaeus* Vero E6 cells [41]. Known examples of altORFs in these species were used to tune the altORF event parameters to a single α, β, γ, δ, and ζ value that can be used across all tested data sets.

With these altORF event parameters, ORFeus correctly identifies well-characterized examples of alternative translation, including: a $+1$ frameshift in *E. coli* prfB (Fig. 4A), a -1 frameshift in SARS-CoV-2 ORF1ab (Fig. 4B), stop codon readthrough in *D. melanogaster* headcase (hdc) (Fig. 4C), uORFs upstream of *S. serevisiae* GCN4 (Fig. 4D), and a dORF downstream of *D. rerio* rrm1 (Fig. 4E). *D. melanogaster* hdc has an abundance of ribo-seq signal in the 5'UTR. With our chosen default parameters, ORFeus does not predict any uORFs to account for this signal, but with slightly different parameter choices it does. We were unable to distinguish whether this signal, which was also recognized by Dunn et al. [16]), represents a real translation signal or some sort of artifact.

These examples show that ORFeus is capable of detecting real altORF events. A subset of these events can be detected in data sets lacking exceptionally clear triplet periodicity (stop codon readthrough in *D. melanogaster*). However, the number of known cases is anecdotal, and it is important to note that the altORF event parameters used to detect these events were optimized for good prediction on these test cases themselves.

Simulated altORFs

To evaluate the performance of ORFeus across a transcriptome, we want to estimate sensitivity and specificity of altORF event detection. Though there are examples of

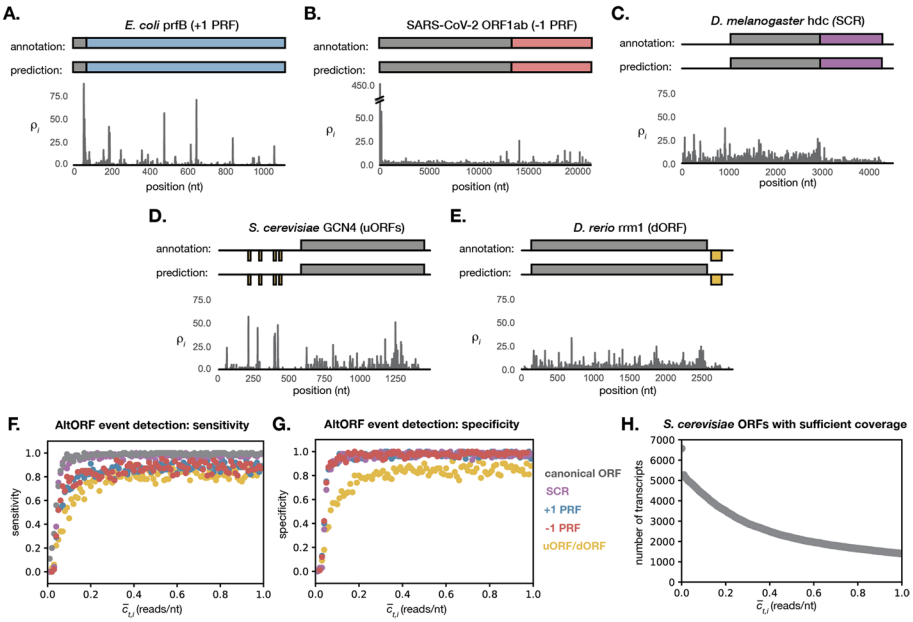

Fig. 4 Model performance on known and simulated altORFs. **A–E** Well-characterized examples of alternative translation events are correctly inferred by the model. The annotated and predicted ORF are shown schematically above the real ρ_i^t signal for each transcript. Sensitivity (**F**) and specificity (**G**) are shown for sequences simulated using parameters estimated from the Wu et al. *S. cerevisiae* data set [38]. Each point represents the mean sensitivity or specificity over 100 simulated sequences with the given mean ribo-seq coverage. **H** The number of ORFs with at least the given ribo-seq coverage drops off rapidly as the coverage threshold increases. The data shown are for the Wu et al. *S. cerevisiae* data set [38]

altORF events across many organisms, there are a limited number of known examples of non-canonical translation represented in any single species. As a result, it is difficult to systematically evaluate the model's performance on all types of altORF events for a single ribo-seq data set. Instead, we devised a method to simulate altORFs from the model. Since an HMM is a generative model, we have the ability to simulate altORFs using the transitions and emissions. We create a state path using the transition probabilities, then select the nucleotide sequence and relative ribo-seq density ρ_i^t values using the emission probabilities for each state.

Sampling from an HMM to generate a simulated ORF is trivial. Here though, we specifically want to simulate altORFs, which include a transition into a specific set of altORF states. Since the probability of transitioning into any given altORF states is rare, we would have to simulate thousands of ORFs from the HMM to generate a single altORF by chance. So instead, we sample *conditional* on the state path including a transition into an altORF event. We use a sampling method that works outward from the desired altORF event. The forward sampling direction follows the standard HMM sequence generation method, but the backward direction depends on a transition matrix inversion (Implementation).

Sequences can also be simulated to have a target mean ribo-seq coverage level $\bar{c}_t$. To do this, we first estimate the total number of reads N_t that should be assigned to the transcript to generate this mean coverage level: $N_t = \bar{c}_t \times L_t$ where L_t is the total length of the transcript in nucleotides. Reads are then assigned to each position i in the transcript with probability proportional to ρ_i^t.

The sensitivity and specificity for altORF detection at different ribo-seq coverage levels were estimated using sequences simulated by this approach (Fig. 4G, H). The model was run on the simulated sequence of nucleotides and relative ribo-seq density values for ORFs of various coverage levels. If an altORF event was simulated and then correctly predicted within $\pm$ 10 nucleotides of the true simulated location, the result was considered a true positive. If no altORF event was simulated, but an altORF event was predicted, the event was considered a false positive.

The ribo-seq coverage level needed for accurate altORF detection will vary by data set. Before running ORFeus on a given ribo-seq data set, we recommend running the sensitivity and specificity simulations (included in the ORFeus code) to determine a coverage threshold that yields appropriate performance (Fig. 4F, G). ORFeus should only be run on transcripts with this ribo-seq coverage or higher. The number of transcripts in a given data set with the necessary coverage level will depend on the coverage threshold chosen (Fig. 4H).

Discussion

Limitations

ORFeus cannot detect translation occurring in more than one reading frame, meaning it is not designed to detect overlapping or internal ORFs. This limitation has important consequences for interpretation of predictions generated by ORFeus. ORFeus may incorrectly predict programmed ribosomal frameshifting events to account for overlapping translation in another reading frame.

ORFeus provides no mechanistic insights about *how* a predicted non-canonical translation event occurs, and is therefore limited in the scope of what types of events can be called. For example, we are unable to distinguish between alternate forms of stop codon readthrough. ORFeus can only identify that there is translation immediately past a stop codon, not whether it is due to selenocysteine incorporation, near-cognate tRNA decoding, or bypassing of the stop codon altogether. All of these events result in downstream in-frame translation past a potential stop codon and are indistinguishable from each other at the current resolution of ribosome profiling data. Similarly, we cannot distinguish a $+1$ programmed ribosomal frameshift from a -2 frameshift (or a -1 frameshift from a $+2$ frameshift), which could result in the same downstream ribo-seq signal. In fact, we even model a -1 frameshift event as a $+2$ frameshift event given the lack of resolution to distinguish between their output, because it is convenient in the structure of the HMM.

Importantly, we limit ourselves to identifying events that could result in pronounced signal changes. For example, we search only for uORFs and dORFs that are translated at a rate comparable to the main ORF, because setting a lower expected signal is more likely to pick up noise. ORFeus is also only capable of predicting frameshifts that generate C-terminally extended protein products (e.g. *E. coli prfB* $+1$ frameshift), since it requires that there be ribo-seq signal in a new frame downstream of the frameshift site. It is unable to identify frameshifts that result in early termination, where little or no sequence is translated in the alternate frame after the frameshift site (e.g. *E. coli dnaX* -1 frameshift). ORFeus is only designed to detect frameshifts with high efficiency (most of the translating ribosomes frameshift and continue translating in the downstream

reading frame). This is because the model only returns the single most likely translation of a transcript. If there is a low efficiency frameshift or an alternate ORF start site that is not used by the majority of translating ribosomes, ORFeus will not detect it.

A final important limitation is that ORFeus cannot distinguish true recoding signals from signals that arise from ambiguous ribo-seq read mapping. Ribo-seq reads from different mRNA isoforms may map to multiple of these isoforms, even though they only truly belong to one. Mismapping of reads from the wrong isoform can lead to apparent changes in reading frame or upstream or downstream translation in the ribo-seq signal. Such signals are not due to true recoding but rather alternative isoforms. This is a long-standing problem in the field of ribo-seq analysis. Alternative isoforms are a critical consideration for eukaryotes that use alternative splicing, and results should be examined to assess whether an alternate isoform might be the cause of any prediction.

Applications

ORFeus can detect several important classes of non-canonical and recoding translation events. Running ORFeus on published or new whole-transcriptome ribo-seq data sets may uncover previously overlooked or unseen translation products. Even in well-annotated genomes, it is likely that alternative protein sequences are translated and have escaped detection by proteomics due to short length or low abundance. For organisms with less well-annotated genomes, ORFeus provides an opportunity to search for both canonical ORFs and non-canonical translation products. However, predictions should be considered with the above limitations in mind and will necessitate additional downstream computational and experimental analysis.

Conclusions

We developed an HMM-based model for inferring both canonically and non-canonically translated ORFs from ribo-seq data. With the ability to detect important types of non-standard translation, ORFeus is a general-purpose tool for uncovering potential novel protein products and expanding our knowledge of translation across different organisms.

Methods

Transcript annotations

Genome sequence and annotations were downloaded for SARS-CoV-2, *E. coli*, *S. cerevisiae, D. melanogaster*, and *D. rerio* from Ensembl [42] (Table 1). Since alternative translation can lead to translation outside of annotated ORFs, it was important to have complete UTR annotations for all species. We updated the annotations and transcript sequences for *E. coli* to include UTRs from RegulonDB [43] and *S. cerevisiae* to include UTRs from Nagalakshmi et al [44].

Ribo-seq data

In order to infer ORFs, ORFeus requires information about the relative density of elongating ribosomes at each position of annotated transcripts. We downloaded raw ribo-seq read data for SARS-CoV-2 infected *C. sabaeus* Vero E6 cells [41], *E. coli* [20], *S. cerevisiae* [38], *D. melanogaster* embryos [16], and *D. rerio* embryos [31]. The

Table 1 Data sources used in this study

Organism	Genome version	SRA accession(s)	Read lengths	P-site offset	P-site position	Ribo-Seq data references
Coronavirus (SARS-CoV-2)	ASM985889v3	SRR12216748-50	28-30nt	5'+14nt	3rd nt	Finkel et al. [41]
E. coli (K12, MG1655)	ASM584v2	SRR4023281	20-40nt	3'-3nt	3rd nt	Hwang and Buskirk [20]
S. cerevisiae (S288C)	R64-1-1	SRR7241903-04	28nt	5'+14nt	3rd nt	Wu et al. [38]
D. melanogaster (embryos)	BDGP6.28	SRR942868-71,74-79	20-40nt	5'+16nt	?	Dunn et al. [16]
D. rerio (embryos)	GRCz11	SRR1062294-302	28-29nt	5'+12nt	1st nt	Bazzini et al. [31]

P-site position indicates the nucleotide of the P-site where most reads map, after the P-site offset is applied. A ? indicates that the periodicity in the data is not clear enough to determine the exact nucleotide within the P-site

SRA accessions used to download each of the raw ribo-seq data sets are shown in Table 1.

We realigned all data sets, since aligned data was not available for many of the studies. This also allowed us to align to the most recent genome version and to offset reads to align to the P-site, which is necessary for correct analysis with ORFeus. Wherever possible, we attempted to replicate the methods used to align the data in the original reference. Each of the raw ribo-seq libraries was processed by: (i) trimming adapters and low quality bases (phred score below 20) with Cutadapt v1.8.1 (Martin, 2011); (ii) removing reads mapping to ladder sequences and organism-specific non-coding RNAs from Ensembl [42]; (iii) aligning remaining reads uniquely to reference genome sequences from Ensembl; (iv) filtering reads by length and offsetting the reads so they correspond to the P-site of the ribosome using Shoelaces [21].

Reads from SARS-CoV-2, *E. coli*, and *S. cerevisiae* were aligned uniquely using Bowtie1 v1.1.1 (-v 2 -y -m 1 -a –best –strata) [45], since few or no introns are present. Reads from *D. melanogaster* and *D. rerio* were aligned using the splice-aware aligner STAR v2.7.0 (–outSAMmultNmax 1 –outFilterMultimapNmax -1 –outFilterMismatchNmax 2) [46] and uniquely mapped reads were identified with Samtools v1.10 (view -h -q 255) [47]. For the offset to the P-site, the exact nucleotide position within the P-site was chosen separately for each data set. Since the model relies on detecting periodicity within an ORF, the precise offset could align the read anywhere within the A-site or P-site. We selected the P-site position that resulted in any distinct start or stop codon signals being mapped to within the start or stop codon respectively, since distinct start and stop signals are explicitly modeled by ORFeus. For example, for the *S. cerevisiae* data [38], we used an offset of 14 nucleotides from the 5' end (which corresponds to the 3rd nucleotide of the P-site) to ensure the distinct stop codon peak mapped within the stop codon (Fig. 1B). However, another offset could be used as long as it still generates a periodic signal within the ORF. Read lengths and offsets selected for each experiment are shown in Table 1.

Parameter estimation

The altORF event parameters were set to the following values: $\alpha = 10^{-5}$, $\beta = 0.5$, $\gamma = 10^{-4}$, $\delta = 10^{-3}$, $\zeta = 10^{-10}$. All other parameters in the model were estimated separately for each ribo-seq data set and corresponding annotations file. Canonical start (AUG), stop (UAA, UAG, UGA), and sense codons were used. Transition probabilities between codons were set to the frequency of each codon in the annotated transcripts. Mean uORF and dORF lengths were set to 50 nts. Mean main ORF lengths were set to the mean ORF length of all annotated transcripts for all data sets.

Sequence simulation

Sequences were simulated by generating a valid state path from the model (using the transition probabilities), then generating valid ribo-seq and nucleotide emissions from each state (using the emission probabilities). For calculation of sensitivity and specificity for rare non-canonical events, sequences were simulated starting at the rare event state(s) and extended in either direction: continuing forward until the end state and backward until the begin state. This was done to ensure the event would be present in the simulated sequence, despite it rarely occurring in normal simulation.

The transition probabilities were used to calculate paths forward during simulation, and the reverse transition probabilities were used to calculate paths backward. Reverse transitions are calculated according to Eq. (1), as outlined by Solow and Smith [48].

$$\begin{aligned} p_{jk} &= P(X_t = k | X_{t-1} = j) \\ q_{jk} &= P(X_t = k | X_{t+1} = j) \\ q_{jk} &= \frac{\pi_k}{\pi_j} p_{jk} \end{aligned} \tag{1}$$

This computation requires that the model meet the conditions of reversibility: stationary (transition matrix doesn't change over time), irreducible (each state can eventually be reached from every other state), positive recurrent (expected return time to each state is finite), and aperiodic (starting in each state, there is no regular period at which the state cannot be reached). These conditions are met for the case where all states are accessible (i.e. α, β, γ, δ, and ζ are all nonzero). π is then the stationary distribution, which is computed by finding the eigenvector for the transpose of the transition probability matrix corresponding to the eigenvalue $\lambda = 1$.

Coverage threshold

The minimum ribo-seq coverage needed to accurately infer altORFs was estimated using simulated sequences. We used the model to generate one hundred sequences per each mean coverage value from 0.01 footprints per nucleotide to 1.0 footprints per nucleotide, in steps of 0.01. To estimate sensitivity, we ran ORFeus on each simulated sequence and determined whether the output Viterbi path contained the correct non-canonical translation event (starting and ending within ± 10 nucleotides of the true simulated positions). For example, a programmed ribosomal frameshift was considered correctly inferred if it was up to 10 nucleotides upstream or downstream

of the true simulated frameshift site. Similarly, a uORF, dORF, or canonical ORF was considered correctly inferred if its start and stop codons were within ±10 nucleotides of the simulated start and stop codons respectively. To estimate specificity, we ran ORFeus on sequences simulated without any altORF events and determined whether the output Viterbi path contained any non-canonical translation event (at any position in the sequence).

Abbreviations

ORF	Open reading frame
altORF	Alternative ORF
uORF	Upstream ORF
dORF	Downstream ORF
SCR	Stop codon readthrough
PRF	Programmed ribosomal frameshift

Supplementary Information

The online version contains supplementary material available at https://doi.org/10.1186/s12859-023-05602-8.

Additional file 1. Complete transition probability matrix for ORFeus. The row label represents the current state, and the column label represents the next state in the path. For example, the probability of transitioning from the begin state to the 5′UTR is shown in the first cell. All blank cells have a transition probability of zero, indicating that there is no probability of transitioning between the corresponding states in the table. The cells containing values each correspond to a transition arrow in Fig. 3A. $L_{5'}$ is the expected length of a 5′UTR in nucleotides; $L_{3'}$ is the expected length of a 3′UTR in nucleotides; L_{ORF} is the expected length of a canonical ORF; L_{sORF} is the expected length of a short uORF or dORF. f_c is the frequency of the next codon in the state path. For example, f_c at the transition from 5′UTR to $start_1$ is the frequency of the next start codon across all start codons (e.g. fraction of start codons that are AUG). Similarly, f_c at the transition from 5′UTR to $start_3$ to $sense_1$ is the frequency of the next sense codon across all sense codons. Note that uORFs and dORFs have the same set of transition probabilities, except that uORFs can begin and end only in a 5′UTR (indicated by "uORF only"), while dORFs can begin and end only in a 3′UTR (indicated by "dORF only").

Acknowledgements
We thank Elena Rivas, Andrew Murray, and members of the Eddy lab for discussions and for feedback on the manuscript. Computations in this paper were run on the FASRC Cannon cluster supported by the FAS Division of Science Research Computing Group at Harvard University.

Author contributions
MOR conceived, designed, and carried out the work under the mentorship of SRE. MOR drafted the manuscript and both authors contributed to and approved the final version.

Funding
MOR was supported by a National Science Foundation Graduate Research Fellowship (DGE 1745303).

Availability of data and materials
All code and data necessary to reproduce and extend the work is freely available at http://eddylab.org/publications/#RichardsonEddy23 and on GitHub at https://github.com/morichardson/ORFeus/releases/tag/v1.0.0.

Declarations

Ethics approval and consent to participate
Not applicable.

Consent for publication
Not applicable.

Competing interests
The authors declare that they have no competing interests.

Received: 24 April 2023 Accepted: 5 December 2023
Published online: 13 December 2023

References

1. Gunišová S, Hronová V, Mohammad MP, Hinnebusch AG, Valášek LS. Please do not recycle! Translation reinitiation in microbes and higher eukaryotes. FEMS Microbiol Rev. 2018;42(2):165–92.
2. Orr MW, Mao Y, Storz G, Qian SB. Alternative ORFs and small ORFs: shedding light on the dark proteome. Nucleic Acids Res. 2020;48(3):1029–42.
3. Ketteler R. On programmed ribosomal frameshifting: the alternative proteomes. Front Genet. 2012;3:242.
4. Atkins JF, Loughran G, Bhatt PR, Firth AE, Baranov PV. Ribosomal frameshifting and transcriptional slippage: from genetic steganography and cryptography to adventitious use. Nucleic Acids Res. 2016;44(15):7007–78.
5. Palma M, Lejeune F. Deciphering the molecular mechanism of stop codon readthrough. Biol Rev. 2021;96(1):310–29.
6. Labunskyy VM, Hatfield DL, Gladyshev VN. Selenoproteins: molecular pathways and physiological roles. Physiol Rev. 2014;94(3):739–77.
7. Firth AE, Brierley I. Non-canonical translation in RNA viruses. J Gen Virol. 2012;93:1385–409.
8. Lawless C, Pearson RD, Selley JN, Smirnova JB, Grant CM, Ashe MP, et al. Upstream sequence elements direct post-transcriptional regulation of gene expression under stress conditions in yeast. BMC Genom. 2009;10(1):7.
9. von Arnim AG, Jia Q, Vaughn JN. Regulation of plant translation by upstream open reading frames. Plant Sci. 2014;214:1–12.
10. Chew GL, Pauli A, Schier AF. Conservation of uORF repressiveness and sequence features in mouse, human and zebrafish. Nat Commun. 2016;7(1):11663.
11. Wu Q, Wright M, Gogol MM, Bradford WD, Zhang N, Bazzini AA. Translation of small downstream ORFs enhances translation of canonical main open reading frames. EMBO J. 2020;39(17): e104763.
12. Taanman JW. The mitochondrial genome: structure, transcription, translation and replication. Biochem Biophys Acta. 1999;1410(2):103–23.
13. Meydan S, Marks J, Klepacki D, Sharma V, Baranov PV, Firth AE, et al. Retapamulin-assisted ribosome profiling reveals the alternative bacterial proteome. Mol Cell. 2019;74(3):481–93.
14. Brierley I, Dos Ramos FJ. Programmed ribosomal frameshifting in HIV-1 and the SARS-CoV. Virus Res. 2006;119(1):29–42.
15. Dinman JD. Programmed ribosomal frameshifting goes beyond viruses. Microbe. 2006;1(11):521–7.
16. Dunn JG, Foo CK, Belletier NG, Gavis ER, Weissman JS. Ribosome profiling reveals pervasive and regulated stop codon readthrough in *Drosophila melanogaster*. eLife. 2013;2: e01179.
17. Loughran G, Chou MY, Ivanov IP, Jungreis I, Kellis M, Kiran AM, et al. Evidence of efficient stop codon readthrough in four mammalian genes. Nucleic Acids Res. 2014;42(14):8928–38.
18. Ingolia NT, Ghaemmaghami S, Newman JRS, Weissman JS. Genome-wide analysis in vivo of translation with nucleotide resolution using ribosome profiling. Science. 2009;324(5924):218–23.
19. Mohammad F, Green R, Buskirk AR. A systematically-revised ribosome profiling method for bacteria reveals pauses at single-codon resolution. eLife. 2019;8: e42591.
20. Hwang JY, Buskirk AR. A ribosome profiling study of mRNA cleavage by the endonuclease RelE. Nucleic Acids Res. 2017;45(1):327–36.
21. Birkeland A, ChyŻyńska K, Valen E. Shoelaces: an interactive tool for ribosome profiling processing and visualization. BMC Genom. 2018;19:543.
22. Raj A, Wang SH, Shim H, Harpak A, Li YI, Engelmann B, et al. Thousands of novel translated open reading frames in humans inferred by ribosome footprint profiling. eLife. 2016;5: e13328.
23. Choudhary S, Li W, Smith A. Accurate detection of short and long active ORFs using Ribo-seq data. Bioinformatics. 2020;36(7):2053–9.
24. Calviello L, Mukherjee N, Wyler E, Zauber H, Hirsekorn A, Selbach M, et al. Detecting actively translated open reading frames in ribosome profiling data. Nat Methods. 2016;13(2):165–70.
25. Crappé J, Ndah E, Koch A, Steyaert S, Gawron D, De Keulenaer S, et al. PROTEOFORMER: deep proteome coverage through ribosome profiling and MS integration. Nucleic Acids Res. 2015;43(5): e29.
26. Verbruggen S, Ndah E, Van Criekinge W, Gessulat S, Kuster B, Wilhelm M, et al. PROTEOFORMER 2.0: further developments in the ribosome profiling-assisted proteogenomic hunt for new proteoforms. Mol Cell Proteom. 2019;18:S126–40.
27. Zhang P, He D, Xu Y, Hou J, Pan BF, Wang Y, et al. Genome-wide identification and differential analysis of translational initiation. Nat Commun. 2017;8(1):1749.
28. Erhard F, Halenius A, Zimmermann C, L'Hernault A, Kowalewski DJ, Weekes MP, et al. Improved Ribo-seq enables identification of cryptic translation events. Nat Methods. 2018;15(5):363–6.
29. Ndah E, Jonckheere V, Giess A, Valen E, Menschaert G, Van Damme P. REPARATION: ribosome profiling assisted (re-) annotation of bacterial genomes. Nucleic Acids Res. 2017;45(20): e168.
30. Ingolia NT, Brar GA, Stern-Ginossar N, Harris MS, Talhouarne GJS, Jackson SE, et al. Ribosome profiling reveals pervasive translation outside of annotated protein-coding genes. Cell Rep. 2014;8(5):1365–79.
31. Bazzini AA, Johnstone TG, Christiano R, Mackowiak SD, Obermayer B, Fleming ES, et al. Identification of small ORFs in vertebrates using ribosome footprinting and evolutionary conservation. EMBO J. 2014;33(9):981–93.
32. Chun SY, Rodriguez CM, Todd PK, Mills RE. SPECtre: a spectral coherence-based classifier of actively translated transcripts from ribosome profiling sequence data. BMC Bioinform. 2016;17(1):482.
33. Ruiz Cuevas MV, Hardy MP, Hollý J, Bonneil E, Durette C, Courcelles M, et al. Most non-canonical proteins uniquely populate the proteome or immunopeptidome. Cell Rep. 2021;34(10): 108815.
34. Zupanic A, Meplan C, Grellscheid SN, Mathers JC, Kirkwood TBL, Hesketh JE, et al. Detecting translational regulation by change point analysis of ribosome profiling data sets. RNA. 2014;20(10):1507–18.
35. Xu Z, Hu L, Shi B, Geng S, Xu L, Wang D, et al. Ribosome elongating footprints denoised by wavelet transform comprehensively characterize dynamic cellular translation events. Nucleic Acids Res. 2018;46(18): e109.
36. Antonov I, Borodovsky M. GeneTack: frameshift identification in protein-coding sequences by the Viterbi algorithm. J Bioinform Comput Biol. 2010;08(03):535–51.

37. Michel AM, Mullan JPA, Velayudhan V, O'Connor PBF, Donohue CA, Baranov PV. RiboGalaxy: a browser based platform for the alignment, analysis and visualization of ribosome profiling data. RNA Biol. 2016;13(3):316–9.
38. Wu CCC, Zinshteyn B, Wehner KA, Green R. High-resolution ribosome profiling defines discrete ribosome elongation states and translational regulation during cellular stress. Mol Cell. 2019;73(5):959–70.
39. Rabiner LR. A tutorial on hidden Markov models and selected applications in speech recognition. Proc IEEE. 1989;77(2):257–86.
40. Viterbi A. Error bounds for convolutional codes and an asymptotically optimum decoding algorithm. IEEE Trans Inf Theory. 1967;13(2):260–9.
41. Finkel Y, Mizrahi O, Nachshon A, Weingarten-Gabbay S, Morgenstern D, Yahalom-Ronen Y, et al. The coding capacity of SARS-CoV-2. Nature. 2021;589(7840):125–30.
42. Howe KL, Contreras-Moreira B, De Silva N, Maslen G, Akanni W, Allen J, et al. Ensembl Genomes 2020-enabling non-vertebrate genomic research. Nucleic Acids Res. 2020;48(D1):D689–95.
43. Santos-Zavaleta A, Salgado H, Gama-Castro S, Sánchez-Pérez M, Gómez-Romero L, Ledezma-Tejeida D, et al. RegulonDB v 10.5: tackling challenges to unify classic and high throughput knowledge of gene regulation in *E. coli* K-12. Nucleic Acids Res. 2019;47(D1):D212–20.
44. Nagalakshmi U, Wang Z, Waern K, Shou C, Raha D, Gerstein M, et al. The transcriptional landscape of the yeast genome defined by RNA sequencing. Science. 2008;320(5881):1344–9.
45. Langmead B, Trapnell C, Pop M, Salzberg SL. Ultrafast and memory-efficient alignment of short DNA sequences to the human genome. Genome Biol. 2009;10(3):R25.
46. Dobin A, Davis CA, Schlesinger F, Drenkow J, Zaleski C, Jha S, et al. STAR: ultrafast universal RNA-seq aligner. Bioinformatics. 2013;29(1):15–21.
47. Li H, Handsaker B, Wysoker A, Fennell T, Ruan J, Homer N, et al. The sequence alignment/map format and SAMtools. Bioinformatics. 2009;25(16):2078–9.
48. Solow AR, Smith WK. Using Markov chain successional models backwards. J Appl Ecol. 2006;43(1):185–8.

Publisher's Note